The Stefan Problem: Polar Exploration and the Mathematics of Moving Boundaries*

J.S. Wettlaufer
Applied Physics Laboratory and Department of Physics
University of Washington, Seattle, Washington 98105-5640
(January 6, 2001)

I. HISTORY

A geophysicist and a mathematician are having coffee. The mathematician queries, "what are you working on these days?" and the geophysicist responds, "I am studying the growth of ice." The mathematician says, "I see, the Stefan Problem!", to which his colleague says, "Oh, so you know about Stefan and Weyprecht?"..."Certainly, Stefan *must* be a mathematician, but Weyprecht–who is Weyprecht?"

We are all keenly aware of the difficulties associated with understanding the subtle aspects of the problems that capture the attention of our colleagues in other disciplines even if those areas historically emerged from the same guiding principles. The disparity between the contemporary mathematical studies of "ice growth", and its origins in polar exploration and Austrian science are the focus of this contribution.

In physics, we know of Josef Stefan as an academic advisor to Ludwig Boltzmann in Vienna. The former is noted for having experimentally discovered, in 1879, the blackbody radiation law which relates the power/area of radiation emitted by an opaque body, P_R, to the absolute temperature T through $P_R = \sigma T^4$, where $\sigma = 5.6703\times10^{-8}$ W m^{-2}K^{-4} is now called Stefan's constant. Boltzmann derived his advisor's relation five years later from statistical mechanics, and it is now called the Stefan-Boltzmann law. This relation is, of course, also of great importance in polar science, allowing us to determine the surface temperature of sea ice by measurement of the emitted radiation, or vice versa.

The seemingly banal phenomenon of the growth of a solid from a cooled boundary comes under the rubric of so-called *Stefan problems*. However, their rich nonlinear behavior, has attracted substantial mathematical interest (e.g. [1]), and their ubiquity in fields ranging from geology to metallurgy stimulates continual rediscovery of Stefan's work, but rarely a scrutiny of its curious history.

It not widely appreciated that Stefan's interest in the thermodynamics of moving boundaries originated with field observations made during various nineteenth century polar expeditions. An interesting question of history concerns precisely which set of observations originally motivated Stefan's consideration of the problem. The curiosity derives from Stefan's pioneering paper of 1889, "Über einige Probleme der Theorie der Wärmeleitung" [2], which begins with a laconic description of the case to be treated:

> Die Probleme, um welche es sich hier handelt, beziehen sich auf solche Fälle, in welchen die Wärmebewegung mit einer Änderung des Aggregatzustandes des Leiters verbunden ist. Die einfachste Aufgabe dieser Art kann in folgender Weise formuliert werden.
>
> Es ist ein Eisprisma gegeben, dessen Temperatur in allen seinen Punkten gleich seiner Schmelztemperatur, also 0 ^{o}C ist. Die eine Endfläche des Prisma wird zur Zeit $t = 0$ mit einer Wärmequelle von der unveränderlichen Temperatur a, welche höher ist als 0 ^{o}C, in dauernde Berührung gebracht.

Essentially, after a cursory comment, Stefan describes the problem of the freezing of a column of ice in contact with a column of water of a higher temperature, with no indication as to his motivation. There is no reference to previous calculations, or to observations or analogies that might have motivated his theoretical analysis. Moreover, his later paper of 1889 which deals with the field data, "Über die Theorie der Eisbildung, insbesondere über die Eisbildung im Polarmeere" [3], was published in the same volume as the theoretical treatment.[1] Today, we are accustomed, or even required, to introduce our papers with a rationale, however tenuous. In fact we know that all studies are prompted by something, a lecture, a conversation, previous attempts by ourselves or other researchers, observations

---

* *Festschrift 150 Jahre Institut für Met. und Geophysik, Univ. Wien*

[1] This paper was originally published in 1889, but was then later published in *Ann. der Physik* in 1891 [4], presumably because this journal enjoyed a wider circulation than the Academy proceedings. It is this later version that is the most often quoted today, largely due to its appearance in the book by H.S. Carslaw and J.C. Jaeger [5]

in the laboratory or in the natural environment, or by the practical need or desire to understand. Perhaps in 1889 rationales or justifications signified a lacking of purity in one's attitude toward science?

We cannot help but wonder the role played in Stefan's thinking by existing field data, and in particular those obtained by Carl Weyprect[2] during the Austro-Hungarian Polar Expedition of 1872-74. The Austro-Hungarian Polar Expedition came under the joint leadership of Julius von Payer[3] and Carl Weyprecht, and according to Payer's classic account published in 1876 [6] all scientific results were turned over to the Austrian Academy of Science, of which Stefan was a member.

In the second paper, mentioned above, published in 1889, Stefan pursues the problem in greater depth and variety, this time including analyses of field observations published in London 1885 and describing observations by various authors at several locations in northern Canada and Alaska between 1829 and 1854, along with observations taken during the Second German North Pole Expedition 1869-70 to the East Greenland Sea. Included in Payer's book is an account of this latter expedition whose scientific results were published in Leipzig in 1874. These include measurements of ice growth and air temperature during the winter. In 1879, Weyprecht, who is generally credited with being the "Father of the International Polar Years" published a substantial book entitled *Die Metamorphosen des Polareises* [7]. Stefan acknowledges Julius von Hann, another Member of the Academy, for having alerted him to the observations made between 1829 and 1870, but there is no reference to the book's of Payer or Weyprecht [3]. Hann was then Director of the Central Institute of Meteorology and Geodynamics, and was a notable pioneer in the field of climatology, which was a natural consequence of his intense passion for the collection, organization and analysis of environmental observations. Therefore, it is rather difficult to believe that Hann, who was clearly in close contact with Stefan, was unaware of relevant data taken during the Payer-Weyprecht expedition. Nevertheless, there is no mention by Stefan [2]- [4] of either their expedition or the relevant data obtained. However, without the benefit of archival studies at the Academy in Vienna one cannot determine whether the data from the 1872-74 expedition contained measurements of ice temperature and growth rate, or any other information that might have aroused Stefan's interest.

Hence, although it appears from his publications that Stefan was unaware of the activities of Payer and Weyprecht, at the very least, the controversy surrounding Payer's departure from Austria would have been known to Stefan, and one would have thought that such a thorough scientist would have sought any additional data that might test his theory?

II. A FEW STEFAN PROBLEMS AND THEIR RELATION TO SEA ICE

A. Stefan's Ocean is Salt Free...

Stefan's one-dimensional, non-fluid-dynamical theory explained many qualititative features of the field data he dealt with. However, he treated the Polar Ocean as a column of pure water, and we know that the salinity of the oceans is a controlling aspect of their dynamics. In order to understand how Stefan could capture much of the behavior of the field data he analyzed, and under what environmental conditions his approach will fail to do so, we begin by summarizing the simplest aspects of his 1889 theory [2].

We imagine that a layer of ice, of instantaneous thickness $z = h(t)$, is in contact with pure water held at the bulk equilibrium melting temperature T_m. The upper boundary of the ice layer is maintained at a temperature $T_B < T_m$ and is located at $z = 0$. In order for ice to grow at the expense of the water below, the latent heat of fusion q_m must be conducted down the temperature gradient through the ice, a necessary consequence of energy conservation described by the flux balance

$$\rho_i q_m \dot{h}(t) = k_i \partial_z T|_{h^-} \qquad \text{at} \qquad z = h(t), \tag{1}$$

known now as the "Stefan condition" wherein the density and thermal conductivity of the solid are given by ρ_i and k_i respectively, q_m is the latent heat of fusion, and $\dot{h}(t)$ denotes differentiation by time (see the review by Worster [8]). The boundary condition at the upper surface of the ice layer is

$$T = T_B \qquad \text{at} \qquad z = 0, \qquad \text{and} \tag{2}$$

the temperature field $T(z, t)$ evolves according to the equation for heat conduction within the ice

[2] C. Weyprecht, 1838-81, Austrian Naval Officer, Explorer

[3] J. Payer, 1841-1915, Austrian Army Officer, Topographer

$$\partial_t T = \kappa_i \partial_{zz} T \qquad \text{in} \qquad h(t) \geq z > 0, \tag{3}$$

where the thermal diffusivity of ice is $\kappa_i = k_i/\rho_i c_i$, in which c_i, is the heat capacity of ice at constant pressure.

The lack of an external length scale in the problem allows this system of equations and boundary conditions to be solved using similarity methods wherein there is a similarity variable $\eta_1 = z/2\sqrt{\kappa_i t}$, the ice thickness is given by

$$h(t) = 2\lambda_1(\kappa_i t)^{1/2} \ , \tag{4}$$

and the temperature field is given by

$$T(\eta) = T_B + (T_m - T_B)\frac{\mathrm{erf}\,(\eta_1)}{\mathrm{erf}\,(\lambda_1)}, \tag{5}$$

wherein $\mathrm{erf}(x) = \frac{2}{\sqrt{\pi}} \int_0^x e^{-y^2} dy$ is the error function. It is the Stefan condition (1) that allows us to complete the solution of the problem, vis-a-vis the transcendental expression

$$S^{-1} = \sqrt{\pi}\lambda_1 e^{-\lambda_1{}^2}\mathrm{erf}\,(\lambda_1)\,, \tag{6}$$

in which the parameter $S = \frac{q_m}{c_i(T_m - T_B)}$ is known as the *Stefan number*, which describes the thermodynamic driving force for solidification: the ratio of the latent heat, to the amount of heat required to cool a region of recently formed solid to the temperature at the upper surface. The development of the solution above is the same, *mutatis mutandi*, as that presented by Stefan in 1889 [2]. The solution of the Stefan condition, Eq. (6), above allows one to predict the thickness and the temperature evolution for a given value of the temperature at the surface of the ice column T_B.

What is now called the quasi-steady approximation [8] was also appreciated by Stefan. Within our contemporary parlance, we ask what happens as the Stefan number becomes large and hence the thermodynamic driving force for solidification becomes small, thereby rendering the temperature field in the solid as quasi-steady. In this case, we can approximate the Stefan condition (1) as

$$\rho_i q_m \dot{h}(t) \approx k_s \frac{(T_m - T_B)}{h}, \tag{7}$$

which is perhaps a more familiar expression whose solution is

$$h \approx \sqrt{\frac{2\kappa_i t}{S}} \qquad \text{whence} \qquad \lambda_1 \approx \sqrt{\frac{1}{2S}}. \tag{8}$$

B. The Polar Oceans are Saline...

It is commonly understood that the freezing point of water is lowered by the addition of salts; for example, salt is dispersed on walkways to melt ice. Perhaps less well appreciated is the fact that the ice lattice efficiently rejects water-soluble impurities. Crudely speaking, when the ocean freezes this phenomenon can result in the enrichment of the water column; an interesting large scale effect originating in a microscopic process. For the present purposes it is sufficient to defer to the empirical understanding that as the concentration of an aqueous salt solution increases, the temperature required to create ice decreases and the ice so created has a lower concentration of salt than does the parent solution. (More detailed discussions can be found elsewhere [9].)

In the limited range of salinities found in the Polar Oceans, the relationship between the equilibrium melting temperature, $T_L(C_L)$, and the bulk salinity of the solution, C_L, is simply $T_L(C_L) = -\ m\ C_L$, wherein m is the *liquidus slope*, that is, the slope of the coexistence line between ice and salt solution. Here m is defined as a positive quantity. The effect of salt rejection by ice is embodied in a *segregation coefficient*; $k_e = C_S/C_L$ which defines the ratio of the salinity of the ice, C_S, to that of the liquid from which it formed C_L. These two effects result in a rich solidification morphology. As ice grows at the expense of salty water, the rejected salt builds up at the growth front thereby enriching the interfacial region. Diffusion and convection can remove the excess salt, but this will take time. Because salt diffuses a hundred times more slowly than heat, the enhanced salinity of the interfacial region may result in it becoming metastable due to the momentary, salinity–induced,reduction in the equilibrium temperature relative to the ambient temperature. This is known as *constitutional supercooling*, and when it is operative fluctuations in the position of the solid–liquid interface will tend to grow at the expense of the supercooled liquid adjacent to the growth front as depicted in figure 1. The interface is then said to be *morphologically unstable* and the growth structure is

a pure solid matrix of ice platelets, with randomly-oriented horizontal c-axes, separated by concentrated brine [9], [10]. This matrix is known in metallurgy as a "mushy layer" [8]. In natural sea ice the impurities primarily consist of salt, but in addition anthropogenic pollution and biological organisms are all concentrated in the interstices between the ice platelets. Under all growth conditions found in the Polar Oceans, the growth is morphologically unstable, leading to the trapping of bulk solution within the two-phase, two-component matrix, or mushy layer. Throughout the remainder of this contribution, we will use the terms mushy layer and sea ice interchangeably.

A major focus in the materials processing of alloys concerns the suppression/control of morphological instabilities. However, in oceanic freezing the concept of controlled growth is not viable; the driving force for solidification persists, and the growth rate of a *mushy layer* must be computed. Interestingly, aqueous solutions have served the metallurgical community as transparent binary alloy analogue systems. Stefan did not deal with the influence of salt. In contrast to Stefan's approach, and many subsequent treatments specific to sea ice over climatological time scales (e.g., [13], [14]) a treatment that includes the influence of morphological instabilities has as a goal to compute, as part of the solution, the amount of liquid in the material. Therefore, it is important to deal with fluid mechanical interactions on scales that are much smaller than typical oceanographic scales, and yet still have geophysical consequences. We initiate intuition with a simplified physical system wherein fluid mechanical interactions are not important. As these effects are added, it will become obvious that the complete problem of sea ice growth contains ingredients that make the task a continuing struggle.

1. "Sea ice" in the absence of gravity

There are six possible fluid dynamical regimes encountered during the solidification of a binary liquid from a horizontal boundary (e.g., [15]). These depend on whether the cooled boundary lies above or below the liquid, and whether the density of the rejected fluid is greater than, less than, or equal to, that of the bulk fluid. First, we consider the case in which a dilute solution of sodium chloride is cooled from below, as would happen for example if the ocean solidified from the sea floor. The fluid adjacent to the upward moving ice front is enriched with solute and is more dense than the bulk fluid. Hence, the stratification of the fluid is stable against buoyancy driven convection, and constitutional undercooling is still controlled solely by molecular diffusion. As is expected from the considerations described above, the system is morphologically unstable, a mushy layer forms and continues to propagate into the melt. The task before us is to calculate both the growth rate of the "sea ice"/solution interface, and the volume fraction of solid within it, given only the initial salinity of the solution and the temperature of the cold boundary from which it is solidifying. Because there are no buoyancy driven motions, it is reasonable to consider that the entire mushy layer is at two-phase coexistence characterized by a constant solid fraction ϕ. Moreover, it is assumed that the solute enriched fluid remains in the interstices of the mushy layer, so that the solute concentration in the bulk fluid remains constant.

The "mushy-layer" equations treat the growing material as a continuum on a scale that is larger than the spacing between ice platelets, but smaller than the characteristic size of the system (e.g., [8]). Just as Stefan considered the thickness of the pure ice layer at any instant in time $h(t)$, we denote the thickness of the mushy layer as $h(t)$. The z direction is normal to the mush/liquid interface, and because the interstitial and bulk fluid are both stably stratified, heat transfer is controlled by diffusion. Moving upward, we formulate a Stefan problem as follows. The lower boundary is held at a temperature T_B that is less than the salinity determined freezing point $T_L(C_L)$,

$$T = T_B \qquad \text{at} \qquad z = 0, \qquad \text{and} \tag{9}$$

the temperature in the layer is described by

$$\partial_t T = \kappa_m \partial_{zz} T \qquad \text{in} \qquad h(t) \geq z > 0, \tag{10}$$

whereas in the intercrystalline liquid the salinity C_L is constrained to solid/liquid coexistence

$$C_L = T/m \qquad \text{in} \qquad h(t) \geq z > 0. \tag{11}$$

The Stefan condition is generalized to include the conductive heat flux in the liquid phase, and the fact that the mushy layer contains a finite volume of liquid,

$$\rho_i q_m \phi \dot{h}(t) = k_m \partial_z T|_{h^-} - k_L \partial_z T|_{h^+}, \qquad \text{at} \qquad z = h(t), \qquad \text{and} \tag{12}$$

the temperature throughout the liquid evolves according to

$$\partial_t T = \kappa_L \partial_{zz} T \qquad \text{and} \qquad C_L = C_\infty \qquad \text{for} \qquad z \geq h(t). \tag{13}$$

The subscript m denotes the values that the heat capacity, c_m, the density, ρ_m, the thermal conductivity, k_m, and the thermal diffusivity, κ_m, take in the mushy layer, described as solid fraction weighted averages,

$$c_m = \phi c_i + (1-\phi)c_L, \tag{14}$$

$$\rho_m = \phi\rho_i + (1-\phi)\rho_L \qquad \text{and} \tag{15}$$

$$k_m = \phi k_i + (1-\phi)k_L, \tag{16}$$

where $k_m = \rho_m c_m \kappa_m$. The conditions that the rejected and enriched fluid must remain in the interstices and at coexistence (Eqs. 11 and 13), have the consequence of leaving the bulk fluid at constant concentration. We can think of this as emerging out of the following process. The motion of the planar ice/solution interface is limited by the slow diffusion of rejected impurities into the bulk fluid. As the salt builds up ahead of the interface and the fluid becomes constitutionally supercooled, the growing corrugations of the unstable interface grow at the expense of the metastable fluid. The newly created mush/liquid interface then moves with a speed that is controlled by *thermal diffusion*, as seen below.

Finally, it is assumed that the increase in solute concentration is achieved by increasing that of the interstitial liquid. This is embodied in the following statement of global solute concentration:

$$h(t)C_\infty = (1-\phi)\int_0^{h(t)} C_L(z,t)dz = m^{-1}(1-\phi)\int_0^{h(t)} T(z,t)dz. \tag{17}$$

The above system of equations, subject to the initial and boundary conditions, that include the condition that the mush/liquid interface lie on the liquidus, admit a similarity solution with

$$\eta = z/2\sqrt{\kappa_L t} \qquad \text{where the interface has height} \qquad h(t) = 2\lambda(\kappa_L t)^{1/2}. \tag{18}$$

The thermal field in the mushy layer obeys

$$T(\eta) = T_B + (mC_\infty - T_B)\frac{\mathrm{erf}\left(\sqrt{\frac{\kappa_L}{\kappa_m}}\eta\right)}{\mathrm{erf}\left(\sqrt{\frac{\kappa_L}{\kappa_m}}\lambda\right)}, \tag{19}$$

and that in the liquid obeys

$$T(\eta) = T_\infty + (mC_\infty - T_\infty)\frac{\mathrm{erfc}(\eta)}{\mathrm{erfc}(\lambda)}. \tag{20}$$

Implementation of the Stefan and global conservation conditions (12) and (17) yields the following pair of simultaneous equations for ϕ and the growth rate λ;

$$\phi^{-1} = 1 - \frac{mC_\infty}{mC_\infty - T_B}\frac{\rho_i}{\rho_L}H\left(\epsilon_m\lambda\right), \tag{21}$$

$$q_m\phi = \frac{c_L(mC_\infty - T_\infty)}{\pi^{1/2}\lambda e^{\lambda^2}\mathrm{erfc}\lambda} + \frac{k_m(mC_\infty - T_B)}{\pi^{1/2}\epsilon_m\lambda e^{(\epsilon_m\lambda)^2}\mathrm{erf}\epsilon_m\lambda}, \tag{22}$$

where $H(x) = (\pi^{1/2}xe^{x^2}\mathrm{erfc}x)(e^{x^2}-1)^{-1}$, $\epsilon_m = \sqrt{D/\kappa_m}$, and D is the solute diffusivity.

This analysis provides a prediction for the growth rate, λ, of a mushy layer of constant solid fraction ϕ determined by the global solute balance. Figure 2 displays the growth rate and solid fraction as functions of C_∞ as compared with the experiments of Huppert and Worster [15], and the prediction that ignores the formation of a mushy layer. We see excellent agreement with the data, and a striking disparity with the prediction ignoring the two phase nature of the mushy layer. A refinement of the theory to allow for the variation of ϕ with space and time further improves the agreement with experiment [17].

The goal for sea ice is essentially the same: to *predict* both the growth rate and solid fraction knowing only the initial salinity of the water and the surface temperature [4]. The growth of sea ice is therefore tantamount to turning the previous problem 'on its head' and solidifying a solution from a horizontal boundary lying above it. The salts increase the density of the interstitial liquid thereby providing the potential energy to drive convection. The convective exchange between the interstitial fluid and the ocean below growing sea ice exerts a controlling influence on the structure of the ice crystals the thereby the overall salt flux delivered to the polar oceans.

A recent experimental study was designed to understand the fundamental role of convection during sea ice growth, and how this extends the the basic theoretical work that can be understood as an addition to the rubric of Stefan problems [11]. The main results demonstrate that the interstitial brine initially remains confined within the sea ice matrix and identify a critical condition for the onset of brine drainage. This underlies the formation of brine channels which are ultimately responsible for the asymptotic structure of sea ice.

The laboratory experiments use aqueous salt solutions as a model for the ocean. Solutions of different initial concentrations of NaCl (ranging from 1 wt.% to 14 wt.%) were placed in a rectangular cell $20 \times 20 \times 28$ cm, the upper boundary of which was cooled to various fixed temperatures (ranging from $-10°$C to $-20°$C) below the liquidus temperature of the solution [11], [12]. In this manner the experimental conditions encompassed typical field conditions. The depth of the mushy layer and the salinity of the liquid below it were measured as functions of time. Finally, the experimental chamber was sealed, and a tube exiting the base led to a graduated burette to record the amount of expansion during solidification as a function of time. This constituted the primary measurement from which the volume of ice grown was determined.

As soon as the mushy layer is formed, weak, distributed compositional convection is observed [11], [12]. However, despite this convection, the concentration of the liquid region below the mushy layer remains constant. After a time, which depends on the thermodynamic conditions of the particular experiment, there is an abrupt change in the character of the convection, which becomes focused into strong, isolated convective plumes (figure 3). It is only after this "internally-driven convection" begins that the concentration of the liquid region (the "ocean") begin to increase, and it does so abruptly, demonstrating a flux of brine from the interior of the mushy layer. The convective plumes emanate from channels in the mushy layer, which have been observed in natural sea ice [10] and in castings of metallic alloys [8], where they are called 'chimneys'.

We can understand the two modes of compositional convection observed in the experiments in terms of a general theory of convection in mushy layers [8]. The theory averages over the microscale of the mushy layer, which is an approach that takes strength from the observation that the circular brine channels observed are not controlled by the plate-like microstructure of the matrix of ice crystals. Thus it appears that the dominant influences in determining channel formation are heat and mass transport coupled with the constraint of two phase equilibrium rather than the crystallographic microstructure of the layer.

Upon consideration of the local mean velocity $\mathbf{u}$, the theory carries in addition the dependent variables of the previous example: local mean temperature T, the local mean salinity of the interstitial liquid C_L, and the local mean solid fraction ϕ. As an expected generalization of Eqs. 10 and 11 the dependent variables are related by equations expressing conservation of heat, salt and momentum vis-a-vis

$$\rho_m c_m \left(\partial_t T + \mathbf{u} \cdot \nabla T\right) = \nabla \cdot (k_m \nabla T) + q_m \partial_t \phi, \tag{23}$$

which is recognized as an advection-diffusion equation for heat, with a source term proportional to the rate of change of the solid fraction and the latent heat per unit mass q_m. This term couples the heat transfer to a salt-conservation equation

$$(1-\phi)\partial_t C_L + \mathbf{u} \cdot \nabla C_L = (C_L - C_S)\partial_t \phi = C_L(1-k_e)\partial_t \phi, \tag{24}$$

in which solutal diffusivity is ignored, because it is much smaller than the thermal diffusivity. It is useful to keep in mind that, in general, the density, ρ_m, heat capacity, c_m, and thermal conductivity, k_m, of the mushy layer are functions of the solid fraction. The momentum equation is written as

$$\mathbf{u} = \Pi(-\nabla p + \rho_m \mathbf{g}), \tag{25}$$

[4]The approach in the sea ice literature is to specify the brine volume profile, i.e., the solid fraction, as derived derived from observation (Reviewed by Leppäranta [14].)

in a form more commonly known as Darcy's equation, describing the flow in a porous medium of permeability Π, which is a function of the local solid fraction ϕ. The latter is determined through the constraint that the mushy layer is in local thermodynamic equilibrium so that the temperature and concentration are coupled by the liquidus relation

$$T = T_L(C_L) = T_B + m(C_L - C_B), \tag{26}$$

rewritten here in a more general form than Eq. (11) where, as above, T_B is the temperature of the cold surface, C_B is the corresponding liquidus concentration and m is the slope of the liquidus. An important point here is that the conservation of heat and salt are coupled to the solid fraction ϕ which makes Darcy's equation one for a *chemically reacting* porous medium. Therefore, the buoyancy term, proportional to the gravitational acceleration $\mathbf{g}$, depends on the local temperature and concentration of the interstitial liquid according to the equation of state

$$\rho_m = \rho_0 \left[1 - \alpha(T - T_0) + \beta(C_L - C_0)\right], \tag{27}$$

where ρ_0, T_0 and C_0 are reference values and α and β are the thermal and solutal expansion coefficients. These equations, more general forms of which can be found in ref. [18], describe the internal evolution of the mushy layer and are coupled through interfacial conditions to the usual equations for heat, solute and momentum conservation in the fully solid and fully liquid regions bounding the mushy layer.

To display the controlling dynamical features of this system it is useful to present the dimensionless expressions, which are obtained by scaling lengths with the thermal diffusion length κ_m/V, times with κ_m/V^2 and velocities with V, where V is the solidification rate, we find for heat conservation

$$\partial_t\theta + \mathbf{u}\cdot\nabla\theta = \nabla^2\theta + S\partial_t\phi, \tag{28}$$

for salt conservation,

$$(1-\phi)\partial_t\theta + \mathbf{u}\cdot\nabla\theta = (\mathcal{C} - \theta)\partial_t\theta, \tag{29}$$

and for momentum

$$\mathbf{u} = -Ra(\nabla p + \theta\mathbf{n}), \tag{30}$$

where

$$\theta = \frac{T - T_B}{\Delta T} = \frac{C_L - C_B}{\Delta C}, \tag{31}$$

$\Delta T = m\Delta C = T_L(C_0) - T_B$ and $\mathbf{n}$ is a unit vector in the vertical direction. The important dimensionless groups are the Stefan number S as shown previously, a compositional ratio

$$\mathcal{C} = \frac{C_s - C_L}{\Delta C}, \tag{32}$$

which describes the difference in composition between the solid and liquid phases relative to the variations in composition of the liquid; and a porous medium Rayleigh number

$$Ra = \frac{g(\beta - \alpha\ m)\Delta C\Pi(\phi)h}{\kappa_L\nu}, \tag{33}$$

which measures the buoyancy force relative to the viscous dissipation in the porous medium. It is the Rayleigh number that principally determines the onset of convection in the mushy layer.

If we solve these equations in the absence of gravity, then the density profile is entirely controlled by the diffusion of salt (figure 4a). In the liquid adjacent to the mushy layer a narrow solutal boundary layer exists in which the density decreases downward. The density drop across the mushy layer itself is of an even greater magnitude, but the proximity of this interstitial liquid to the confining solid crystals results in a greater resistance to flow. The stability to convective motions of this configuration was assessed by Worster [18] who predicted a stability boundary (figure 4b) with two possible modes of convection: one driven by the buoyancy in the compositional boundary layer; the other driven by the buoyancy internal to the mushy layer. In figure 4c the streamlines corresponding to these two modes of convection are shown, the relative stability of which varies with the parameters of the system. In the case of laboratory simulations of sea ice growth we find that the boundary-layer mode is the first to become unstable. The distinction between these two modes is dramatic. The boundary-layer mode is characterized by small length scales and is not sufficiently vigorous to penetrate to any great extent into the mushy layer. For this reason, it is responsible

for only a very small salt flux, and most of the enriched brine is trapped in the interstices of the mushy layer. The potential energy stored in the interstitial brine throughout the layer is released by the mushy-layer mode of convection and is thereby responsible for the much larger flux of salt observed in the laboratory. As is shown below, this mode of instability is initiated when the Rayleigh number exceeds a critical value R_c.

The mushy-layer mode of convection is also responsible for the initial formation of brine channels, which form the principal routes for the desalination of sea ice [9], [10]. The mechanism is as follows. Prior to the onset of this mode of instability, the interstitial liquid in a mushy layer is in local thermodynamic equilibrium, and hence the colder liquid near the cooled boundary is also saltier. If a parcel of liquid within the mushy layer displaced downward, away from the cold boundary, it comes into contact with surrounding material that is warmer and fresher. Due to the substantially smaller relaxation time for temperature relative to salt, the displaced parcel comes into thermal equilibrium without a significant change in its salinity. Hence, the displaced parcel is oversaturated in salt and, in order to restore local equilibrium, will partially dissolve the nearby ice crystals. Therefore, in regions where the flow is directed along the temperature gradient and away from the cold boundary, the solid phase will dissolve. By parity of reasoning, upward flow, toward the cold boundary, will result in solidification of ice. This asymmetry between up and down flow, and the associated solidification and dissolution of ice creates inhomogeneities in the permeability, and focuses the convective flow into narrow channels that are observed to form during the stages of growth following the onset of internally-driven convection.

Testing of the hypothesis that internally-driven convection and the concomitant formation of brine channels is initiated once the Rayleigh number exceeds a critical value is equivalent to testing the degree to which the scaling

$$(h_c \Delta C)^{-1} \propto \Pi(\phi_c), \tag{34}$$

is obeyed experimentally. Here, h_c is the critical depth of the mushy layer, and ϕ_c is the corresponding vertically averaged solid fraction. In figure 5 we plot $(h_c\Delta C)^{-1}$ as a function of the critical liquid fraction, $1-\phi_c$, for all thirteen experiments [12]. The collapse of the data is excellent. Moreover, the functional form of the relationship between $(h_c\Delta C)^{-1}$ and $1-\phi_c$ is consistent with the expected form of the permeability function Π, the latter increasing with the liquid fraction and having positive curvature. We can view this collapse either as an empirical marginal stability diagram, or as a dynamic phase diagram for convection, which shows the conditions under which brine will drain from a mushy layer.

C. The Geophysical Relevance

The formation of brine channels has a significant impact on the structure of the mushy layer and on the convective exchange between the mushy layer and the underlying liquid. Because the brine draining through channels in the mushy layer is replaced by fresher liquid from below, the return flow drives further growth of ice in the layer, thereby increasing its solid fraction, which is seen as a systematic feature associated with the onset of internally driven convection. Because the thermal, acoustic, electromagnetic, mechanical and biological properties of sea ice are all influenced by the solid fraction, such abrupt changes are of broad interest.

Open water and thin sea ice play an important role in the surface heat and mass balance of the Arctic Ocean. In the wintertime, divergence in the wind stress generates cracks in the ice cover, known as leads, which expose the ocean to a cold atmosphere, thereby driving rapid solidification and large heat and salt fluxes. These local events can create large-scale oceanic and atmospheric phenomena, and hence the community has focused a great deal of effort in the study of the processes that accompany lead formation. The approach described in the previous section has been brought successfully to bear on field data taken during the formation and evolution of a lead. This was done by analyzing highly resolved temperature data taken through the air/sea/ice interface. As predicted theoretically and shown experimentally as described above, it was found that haline convection, driven from within growing sea ice is initiated during the same time period as observed by direct oceanographic measurements. The geophysical importance of this process is that, although ice growth is continuous, the brine flux commences abruptly, only after some time, and this finding is in contrast to what had previously been supposed. Therefore, a proper treatment of the phase dynamics of sea ice growth is crucial for a quantitative understanding of the brine flux delivered to the surface of the ocean. Furthermore, we found that, in this particular situation, during intervals in which the surface temperature decreases with time, the sea–ice growth is a linear function of time, in contrast to the model typically used in numerical simulations. The most practical methods of studying lead convection are numerical simulations and laboratory models, and hence a strong conclusion of this approach concerns the quantitative treatment of the boundary conditions describing the buoyancy flux.

Another basic aspect of the heat and mass balance in ice-covered seas concerns the distribution of ice thickness [20] which deals with the three dimensional morphology of the ice cover as it grows, decays and deforms. The aspect

that involves the phase dynamics of young ice concerns its interaction with the oceanic boundary layer. Because the hydraulic roughness of sea ice influences the boundary-layer dynamics, it must also influence the heat and mass fluxes at the ice-ocean interface. Therefore, uncovering potential mechanisms that underlie an increase or decrease of the hydraulic roughness of sea ice is of geophysical relevance. In young sea ice, a sufficiently rapid oceanic flow can give rise to the creatiion of a corrugated sea-ice-ocean interface [21], [22]. The mechanism relies on the flow of brine developing within sea ice in response to Bernoulli suction caused by boundary layer flow adjacent to the interface. The resulting corrugation wavelength is approximately three to four times the thickness of the sea ice and hence, for relatively thin ice, will have a substantial influence on the hydraulic roughness. Moreover, the evolution of a rough ice-ocean interface can trigger buoyancy-driven circulation within sea ice by bringing dense brine to the same depth as less dense ocean water. Detailed analyses show that such circulations can ultimately create brine channels. The conditions in which instability is most likely operative are found during storms in the central Arctic Ocean, in ice-covered tidally driven fjords, or in coastal polynyas where the magnitude of the wind drift is large.

III. EPILOGUE

What then of Stefan? We have seen that Stefan's 1889 theory was eventually used in the analysis of data obtained in a number of expeditions with the exception of that taken during the Austro-Hungarian Polar Expedition of 1872-74, mounted by his contemporaries Julius von Payer and Carl Weyprecht. Although these data were delivered to the Austrian Academy, Stefan could nonetheless have been unaware of their existence? Perhaps the data were not in a form convenient or suitable for analysis? Finally, it is possible that the theory did not adequately capture the features of the data?

Were this latter issue to be of relevance one can imagine at least one well known geophysical phenomenon that would play an important role: the heat flux from the ocean. The treatment of the heat flux from the liquid phase in the boundary condition (12) assumes that the mechanism of one of molecular conduction. However, under floating sea ice, this flux is a turbulent quantity and the evolution of the ice thickness is extremely sensitive to its magnitude [13] and geographic variation [23], [24]. Indeed, in the northeastern Barents Sea, where the Tegethoff drifted, there may well have been relatively warm water masses from the North Atlantic. On the contrary, the ocean heat flux from the East Greenland current, the location of the earlier ice growth observations, was likely to be very small [25], thereby more closely matching Stefan's calculations. If the Payer/Weyprecht expedition encountered a relatively large oceanic heat flux, it would have shifted the dominant interfacial energy balance and would have led to a poor comparison between theory and observation. Although this is a reasonable speculation, based on our contemporary understanding of this phenomenon, it is speculation nonetheless. Archival studies would go a long way toward putting this in context.

Independent of this latter point, what we see in Stefan's original work are the important ingredients of a problem that has burgeoned into many avenues, but avenues that still maintain the core structure that he layed out. Such a characteristic defines important advances in science.

IV. ACKNOWLEDGMENTS

It is a pleasure to thank Norbert Untersteiner, who initiated my interest in sea ice, stimulated this contribution, insured an accurate interpretation of Stefan's papers, and made the process an enjoyable one. Grae Worster kindly read the penultimate version of the manuscript and helped improve both my thinking on the topic, and the submission. My research on the phase changes in water systems is generously supported by the US Office of Naval Research and National Science Foundation.

---

[1] Meirmanov, A.M., *The Stefan problem*, (W. De Gruyter expositions in mathematics, Berlin, 1992).

[2] J. Stefan, 1889, "Über einige Probleme der Theorie der Wärmeleitung", *Sitzungsberichte de Mathematisch–Naturawissenschaftlichen Classe der Kaiserlichen, Akademie der Wissenschaften* **98**(2a), p. 473-84.

[3] J. Stefan, 1889,"Über die Theorie der Eisbildung, insbesondere über die Eisbildung im Polarmeere", *Sitzungsberichte de Mathematisch–Naturawissenschaftlichen Classe der Kaiserlichen, Akademie der Wissenschaften* **98**(2a), p. 965-83.

[4] J. Stefan, 1891,"Über die Theorie der Eisbildung, insbesondere über die Eisbildung im Polarmeere", *Ann. der Physik u. Chem., Neue Folge* **42**, p. 269-86.

[5] Carslaw, H.S., and Jaeger, J.C., *Conduction of Heat in Solids* (Clarendon, Oxford, 1959).
[6] J. Payer, 1876. Die Oesterreichisch-Unhgarische Nordpol-Expedition in den Jahren 1872-1874, 696 pp., (Alfred Hoelder, Wien).
[7] C. Weyprecht, 1879, *Die Metamorphosen des Polareises* 284 pp., (Perla Verlag, Wien).
[8] M.G. Worster, 2000 "Solidification of Fluids", in *Perspectives in Fluid Dynamics*, eds. G.K. Batchelor, H.K. Moffatt & M.G. Worster, (Cambridge Univ. Press, Cambridge)
[9] J.S. Wettlaufer, 1998, "Introduction to Crystallization Phenomena in natural and artificial sea ice", in *Physics of Ice-Covered Seas*, edited by M. Leppäranta, (University of Helsinki Press, Helsinki, 1998), p. 105-194.
[10] W.F. Weeks, 1998, "Growth conditions and the Structure and Properties of sea ice", in *Physics of Ice-Covered Seas*, edited by M. Leppäranta, (University of Helsinki Press, Helsinki, 1998), p. 25-104.
[11] J.S. Wettlaufer, M. G. Worster, and H. E. Huppert, 1997a, "The phase evolution of young sea ice", *Geophys. Res. Lett.* **24**, p. 1,251-1,254.
[12] J.S. Wettlaufer, M. G. Worster, and H. E. Huppert, 1997b,"Natural convection during solidification of an alloy from above with application to the evolution of sea ice", *J. Fluid. Mech.*, **344**, p. 291-316.
[13] G. A. Maykut and N. Untersteiner, 1971, "Some results from a time dependent thermodynamic model of sea ice", *J. Geophys. Res.* **76**, p. 1,550-1,575.
[14] M. Leppäranta, 1993, *Atmos.-Ocean* **31**, p. 123-38.
[15] H.E. Huppert and M.G. Worster, 1985, "Dynamic solidification of a binary melt", *Nature* **314** p.703-7.
[16] H.E. Huppert, 1990, "The fluid mechanics of solidification", *J. Fluid Mech.* **212**, p. 209-40 (1990).
[17] M.G. Worster, 1986, "Solidification of an alloy from a cooled boundary", *J. Fluid Mech.* **167**, p. 481-501.
[18] M.G. Worster, 1992, "Instabilities of the liquid and mushy regions during solidification of alloys", *J. Fluid Mech.* **237**, p. 649-69.
[19] J.S. Wettlaufer, M. G. Worster, and H. E. Huppert, 2000, "Solidification of leads: Theory, experiment, and field observations", *J. Geophys. Res.* **105** p. 1,123-1,134.
[20] A.S. Thorndike, 1992, "Estimates of sea ice thickness distribution using observations and theory" *J. Geophys. Res.* **97** p.12601-5.
[21] D.L. Feltham, and M. G. Worster, 1999, "Flow-induced morphological instability of a mushy layer", *J. Fluid Mech.*, **391**, p. 337-357.
[22] D.L. Feltham, M. G. Worster, and J. S. Wettlaufer, 2000, "The influence of ocean flow on newly-forming sea ice", (subjudice) *J. Geophys. Res.*.
[23] J.S. Wettlaufer, 1991, "Heat flux at the Ice-Ocean interface" *J. Geophys. Res.* **96** p. 7215-36.
[24] N. Untersteiner, 1988, "On the ice and heat balance in Fram Strait" *J. Geophys. Res.* **93** p.527-31.
[25] M.G. McPhee and N. Untersteiner, 1982, "Using sea ice to measure vertical heat flux in the ocean" *J. Geophys. Res.* **87** p.2071-4.

FIG. 1. Schematic of constitutional undercooling, and its potential for creating morphological instabilities. On the left side of the figure we plot the profile in the z-direction of the actual temperature, T, and the liquidus temperature, $T_L(C_L)$, and on right side we plot the profile of the solute concentration, C_L, which equals the far field value, C_∞. On the top we plot the equilibrium configuration (growth speed $V = 0$) that is isothermal (left) and at constant composition, where C' equals the far field value, C_∞ (right), so that $T_L(z) = T(z)$. Below, during growth at constant speed V solute build up adjacent to the moving front (right) can local depress the freezing point $T_L(z)$ (now seen as the dashed line) below the actual temperature, $T(z)$ (left). We show examples of two different imposed temperature profiles, T_a and T_b. The latter is the profile responsible for constitutional undercooling because in a region adjacent to the interface, the actual temperature is less than the temperature at which solid will form at the local solute concentration.

FIG. 2. Plots of growth rates (λ's) and solid fraction (ϕ) as functions of C_0, as compared to the experiments of Huppert & Worster (1985). The prediction that ignores the morphological instability is the lower curve denoted by λ, and that which includes it is denoted by λ_m (adapted from Huppert, 1990). Note the striking disparity with the prediction that ignores the two phase nature of the mushy layer, i.e., ignores the morphological instability: The agreement with the data (the X filled circles) is excellent for λ_m, & Worster (1986) further improved the agreement by considering the evolution of ϕ.

FIG. 3. Results for an experiment with initial concentration $C_0 = 3.55$ wt.% NaCl and temperature at the upper surface $T_B = -20°$C. (a) The measured concentration of the liquid region as a function of thickness of the mushy layer and a curve drawn to fit the measurements. The concentration remains constant initially, indicating that brine rejected by the growing ice remains in the mushy layer. Once the thickness of the mushy layer exceeds a critical value h_c, brine drains into the underlying liquid region. (b) The evaluated solid fraction of the mushy layer as a function of time. The mushy layer begins to grow more slowly once the critical thickness has been exceeded since the increased solid fraction requires the removal of additional latent heat. (Adapted from Wettlaufer, Worster & Huppert 1997a,b.)

FIG. 4. (a) The diffusion-controlled density profile in the absence of convection is unstably stratified throughout the mushy layer, of thickness $h(t) < h_c$, and in a narrow compositional boundary layer ahead of the mush–liquid interface. A linear stability analysis [18] determines the neutral curve (b): when the Rayleigh number is larger than the values given by the neutral curve convection will occur. The two minima of the neutral curve correspond to two different modes of convection. The boundary-layer mode typically occurs first (at lower Rayleigh numbers) and gives rise to convection of a limited extent in the liquid region, as shown by the streamlines (c). When the mushy layer is deeper, the Rayleigh number is larger and the mushy-layer mode of convection is triggered. This mode penetrates the full depth of the mushy layer.

FIG. 5. Critical conditions for the onset of a significant brine flux from the mushy layer. Crosses show when the brine flux began in each experiment. The initial concentration in the experiments ranged between 1 and 14 wt.% NaCl. The surface temperature ranged between -10 and -20°C. When the conditions of the mushy layer lie above the marginal curve drawn through the data, most of the salt rejected by the growing ice remains trapped in the mushy layer. Once the conditions of the mushy layer lie below the marginal curve then brine will be convected out of the mushy layer. Note the adherence to the Kozeny form for permeability function. We view this as a semi-empirical marginal stability diagram. (Adapted from Wettlaufer, Worster & Huppert 1997a,b.)

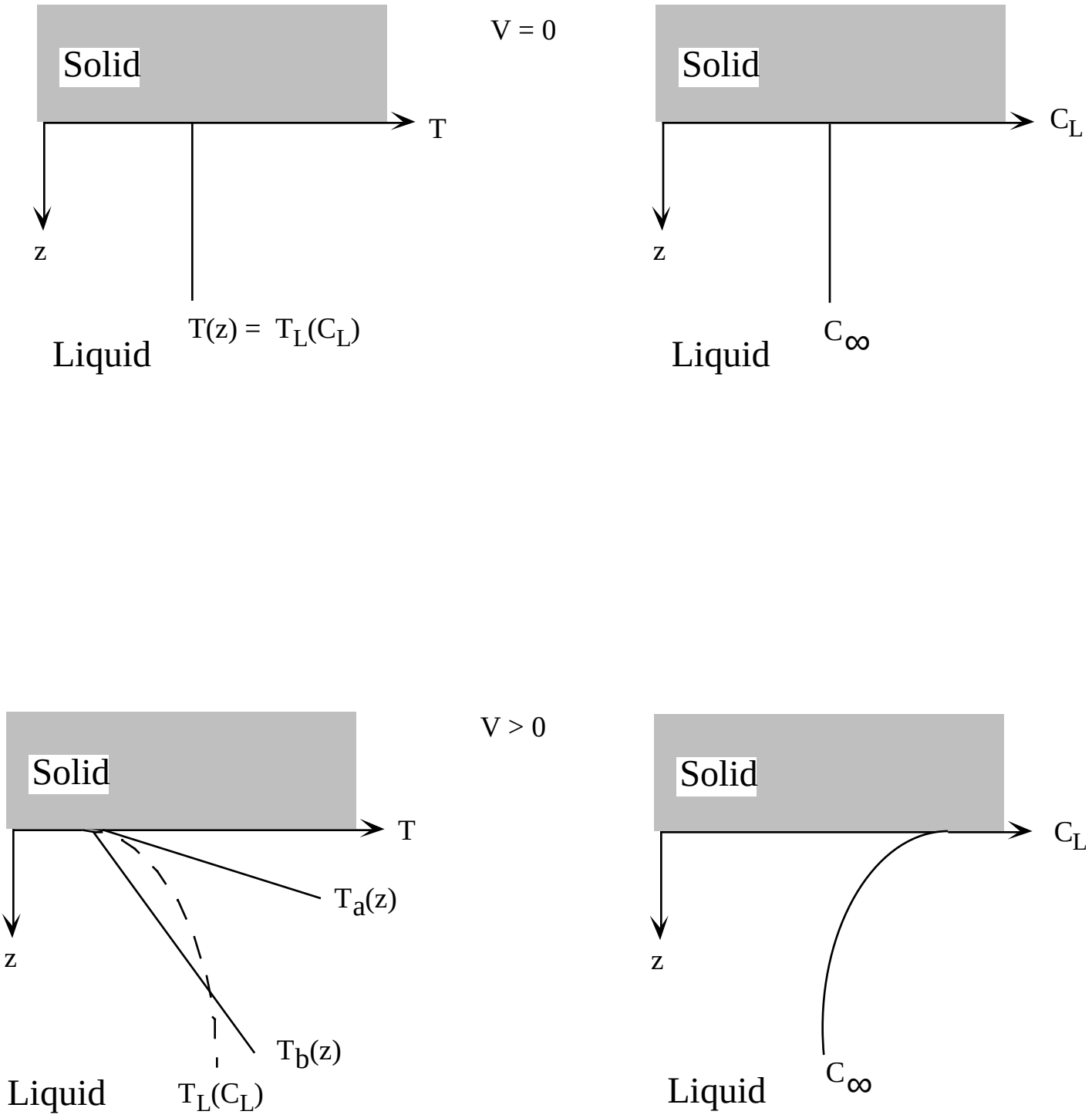
V = 0
Solid
T
z
T(z) = T_L(C_L)
Liquid
Solid
C_L
z
C∞
Liquid
V > 0
Solid
T
T_a(z)
z
T_b(z)
Liquid
T_L(C_L)
Solid
C_L
z
C∞
Liquid

Fig. 1

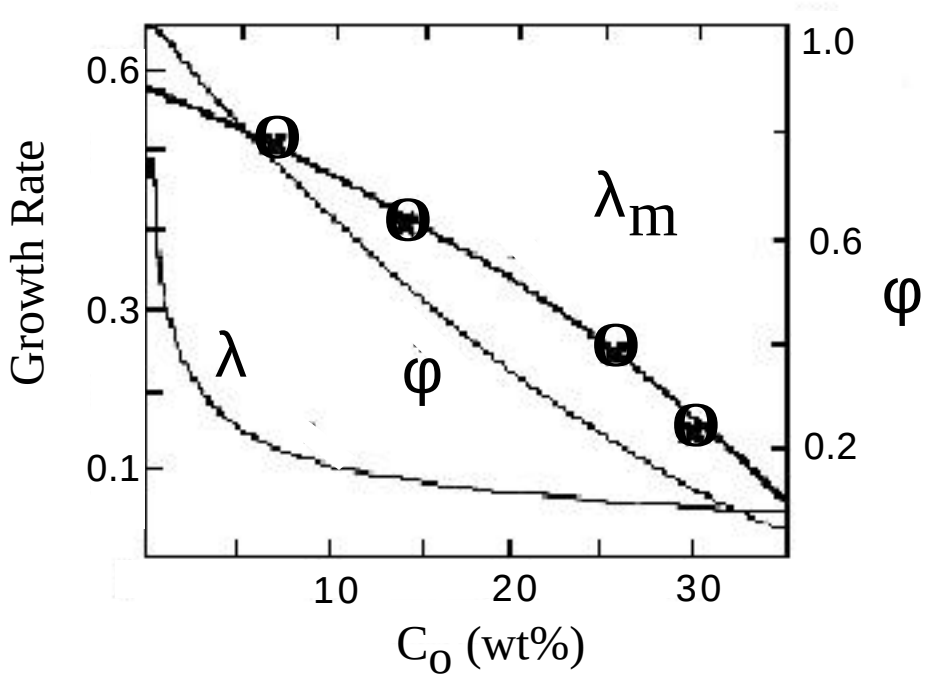

Fig. 2

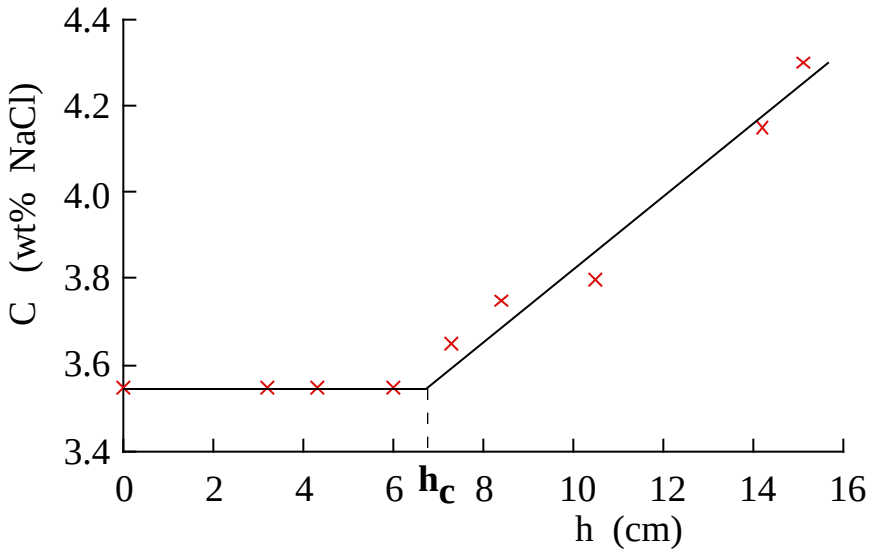

Fig. 3(a)

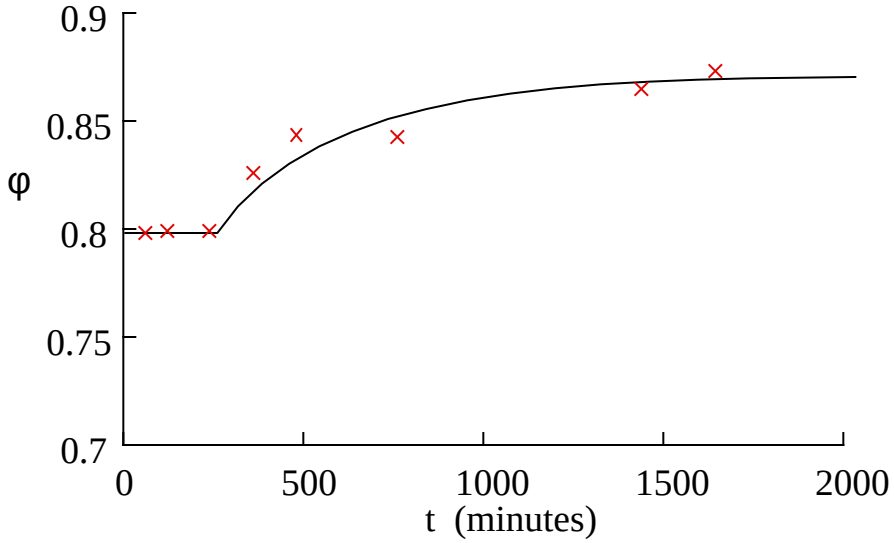

Fig. 3(b)

$\frac{1}{h_c \Delta C}$ $(cm^{-1}\, wt.\%^{-1})$

Fig 5.

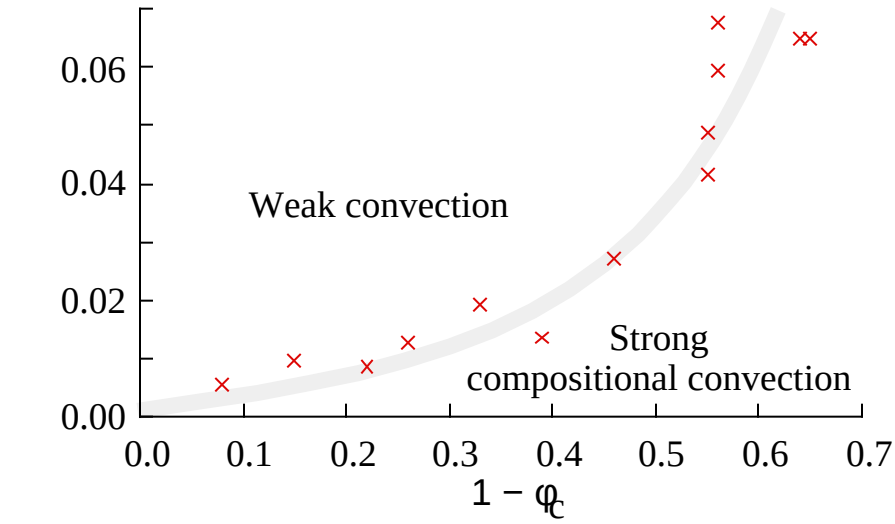

Fig. 4

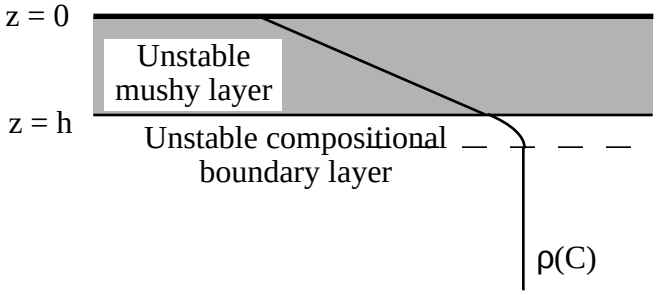
z = 0
z = h
Unstable
mushy layer
Unstable compositional
boundary layer
ρ(C)

(a)

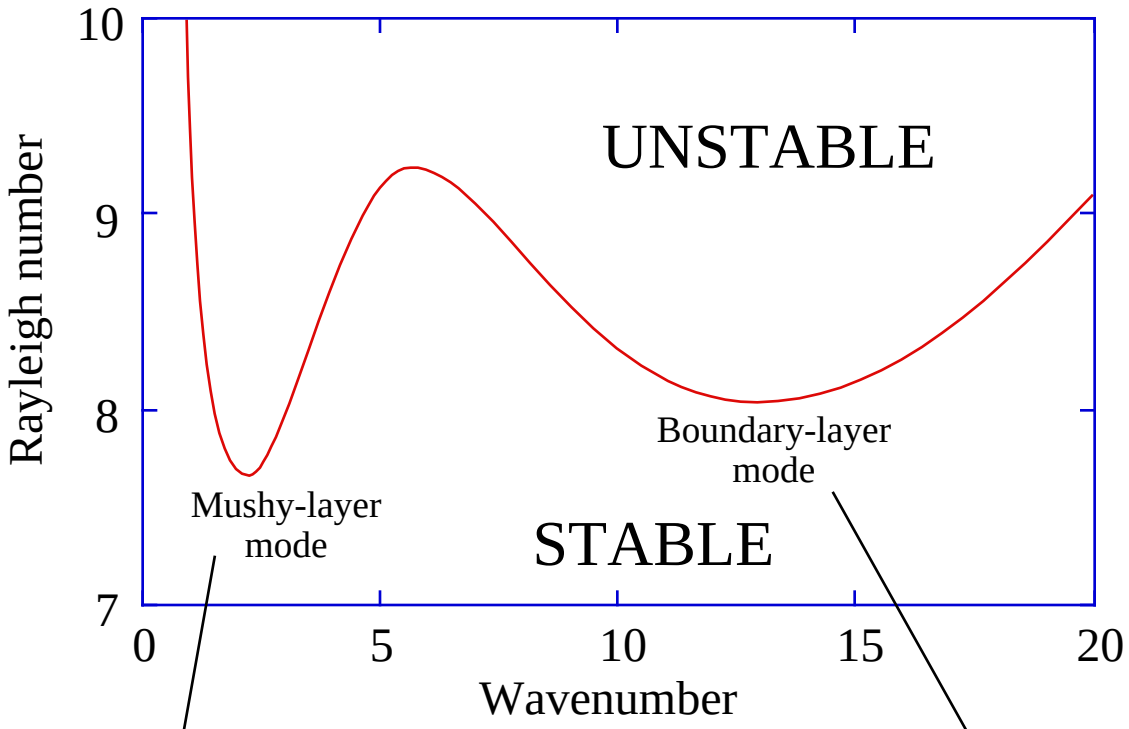
10
9
8
7
Rayleigh number
UNSTABLE
STABLE
Mushy-layer
mode
Boundary-layer
mode
0
5
10
15
20
Wavenumber

(b)

(c)

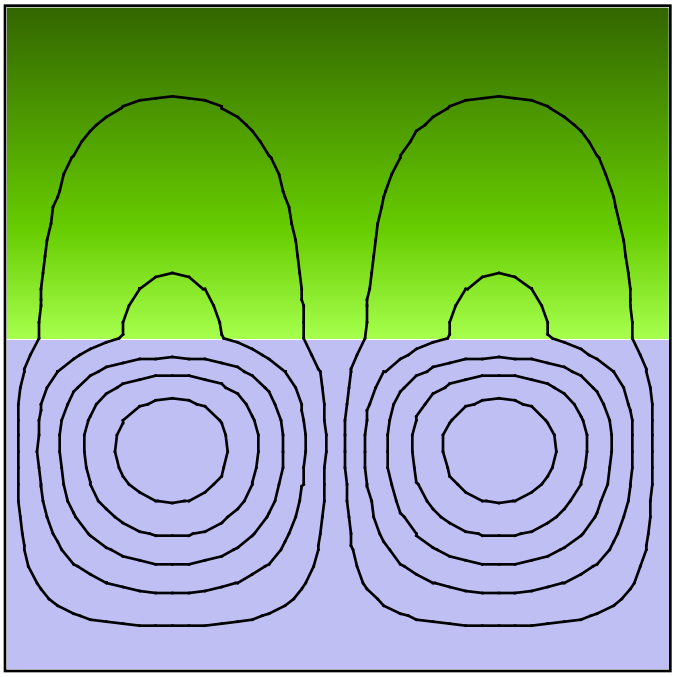

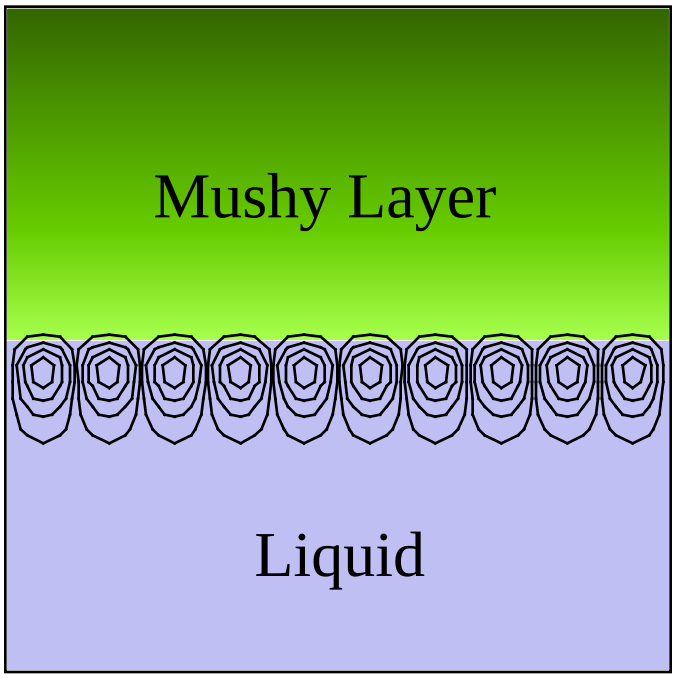
Mushy Layer
Liquid